Fall 12-20-2019

Reliability Sensitivity Analysis of Dropped Objects Hitting on the Pipeline at Seabed

Hanqi Yu
hyu4@uno.edu

Reliability Sensitivity Analysis of Dropped Objects Hitting on the Pipeline at Seabed

A Thesis

Submitted to the Graduate Faculty of the
University of New Orleans
in partial fulfillment of the
requirements for the degree of

Master of Science
in
Engineering
Naval Architect and Marine

by

Hanqi Yu

B.S. Shanghai Maritime University, 2018

December 2019

Acknowledgement

I would like to take this opportunity to express my deep gratitude to my Professor, Dr. Vincent Xiaochuan Yu, who has offered me constructive guidance for the planning of the thesis and invaluable advice and encouragement for its completion and improvement.

Besides, I wish to extend my sincere gratitude to Dr. Brandon Taravella and Dr. Lothar Birk, who serve as my thesis committee and provide me numerous help in my study at School of Naval Architecture and Marine Engineering, University of New Orleans. Especially, I sincerely appreciate Dr. Linxiong Li in Math Department for his guide in reliability and statistics.

Finally, I am deeply indebted to my beloved parents and friends, who have always supported me, willingly discussed the problems with me, and offered valuable insights.

Table of contents

List of Figures

List of Tables

Nomenclature

$\boldsymbol{X}$	Horizontal position at the seabed (m)
δ	Lateral deviation (m)
$p(X)$	Probability of a dropped object landing at position X
d	Water depth (m)
$\boldsymbol{Y}$	Horizontal position along Y direction (m)
r	Absolute excursion on the seabed (m), defined as $\sqrt{X^2 + Y^2}$
$p(r)$	Probability of a dropped object landing at excursion r
A_r	Ring area (m^2)
r_i	Inner radius (m)
r_o	Outer radius (m)
$P_{hit,r}$	Probability of hit within A_r with r_i and r_o
P_{hit,A_r}	Conditional probability of hit per seabed area
$P_{hit,\mathrm{sl,r}}$	Probability of hit to a subsea line within a certain ring
L_{sl}	Length of subsea line within the ring (m)
D	Diameter of subsea line (m)
B	Breadth of falling object (m)
β	Instantaneous rotational angle between x-axis and X-axis
U_1	Velocity component for surge
U_3	Velocity component for heave
Ω_2	Velocity component for pitch
M_{55}	Moment of inertia in pitch direction
m_{33}	Added mass for heave motion from strip theory
m_{55}	Added mass for pitch motion from strip theory
m_t	2D added mass coefficient for heave direction at the trailing edge
x_t	Longitudinal position of effective trailing edge
∇	Volume of the cylinder
ν	Kinematic viscosity of water
$\mathrm{C_{dx}}$	Drag coefficient in x-direction
$\mathrm{C_{dz}}$	Drag coefficient in z-direction
$F_{hit,\mathrm{sl,r}}$	Frequency of hit to the subsea line within a certain ring (per year)
N_{lift}	Number of lifts (per year)

f_{lift}	Frequency of drop per lift (per year)
m_p	Plastic moment capacity of the wall ($=\frac{1}{4}\sigma_y t^2$) (N)
δ_1	Pipe deformation (or dent depth) (m)
t	Wall thickness (m)
σ_y	Yield stress (N/m^2)
D_0	Steel outer diameter (m)
E_S	Dent- absorbed energy for steel pipelines (J)
E_E	Kinetic energy (J)
E_T	Terminal energy (J)
E_A	Energy of added hydrodynamic mass (J)
E_C	Concrete coating energy (J)
E_{C1}	Concrete coating energy for long/flat shaped objects (J)
E_{C2}	Concrete coating energy for box/round shaped objects (J)
E_P	Polymer coating energy (J)
m	Mass of dropped object (kg)
V	Volume of dropped object (m^3)
ρ	Density of seawater (kg/m^3)
A	Collision area (m^2)
C_D	Drag coefficient
C_a	Added mass coefficient
Y	Crushing strength (N)
B	Width of the dropped object (m)
x_0	Penetration depth (m)
h	Height of dropped objects (m)
G	Limit state function
L	Load that can be withstood by the property of the pipeline itself
S	Impact strength that comes from the dropped object
σ	Standard deviation regardless of the subscript
$P_{f,damage}$	Probability of damage

$\widetilde{P}_f(\theta, \sigma)$	Probability of failure
$f_X(\boldsymbol{x})$	Joint probability density function
$\boldsymbol{x}$	An n-dimensional vector of random variables described by $f_X(\boldsymbol{x})$
$D(x)$	The set of all n-tuples of real numbers
ϕ	Cumulative distribution function
θ	The parameter to which sensitivity analysis is performed

Abbreviation

DNV	Det Norske Veritas
DROBS	Dropped Objects Simulator
EOM	Equations of Motion
2-D	Two dimensional
3-D	Three dimensional
CV	Coefficient of variation

Abstract

Nowadays, as oil industry gradually moves towards deep sea fields with water depth more than 1000 meters, they are subjected to several threats which can cause failure of the pipeline, of which the accidentally-dropped objects have become the leading external risk factor for subsea developments. In this thesis, a sample field layout introduced in Det Norske Veritas (DNV) guide rules is selected as the study case with 100m water depth. Six different groups of dropped objects are used in this paper. The conditional hit probability for long/flat shaped objects will be calculated with the methods from both DNV rules and an in-house tool **Dr**opped **Ob**jects **S**imulator (DROBS). The difference between the results will be discussed. Meanwhile, the sensitivity analysis on mass (M), collision area (A), the volume (V), added mass coefficient (C_a) and drag coefficient (C_d) of the objects are calculated.

Keywords: dropped objects, DNV, probability of failure, sensitivity analysis, Monte Carlo Simulation

I. Introduction

Subsea pipelines are one of the most economic and reliable means of transporting hydrocarbons. However, in remote areas, they may be susceptible to leakage and rupture due to unavoidable factors (Y. Yang et al. 2016). Not to mention that the leakage of oil will have a great influence on the ocean environment and cause significant repair costs. One of the simplest ways to estimate the failure frequency is to look at statistically incident records as shown in Fig. 1, from which third-party damage and corrosion constitute are the most important risk factors, accounting for 38% and 36% respectively. As the impact of dropped objects can be viewed as a genre accounting for the third-party damage, accidentally dropped objects from a platform deck or from a supply vessel or during a hoisting operation may cause fatal casualties. Therefore, to protect the subsea system, it is necessary to estimate the hit probability of the accidentally-dropped objects on the seabed as well as the sensitivity analysis of some important parameters.

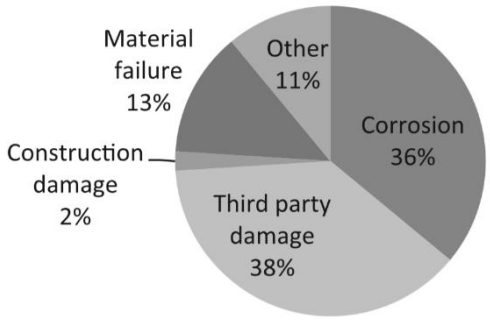

Figure 1 Cause distribution of subsea pipeline failure (Yang et al 2016)

In recent years, several analysis methods have been proposed on offshore risk assessment. Begg et al. (1992) described an analysis methodology in which cumulative impact frequencies over a subsea grid element give impact scatter diagrams, impact contour maps and three-dimensional (3D) impact probability density functions. Luo et al. (1992) focused on the transient motion of dropped objects during offshore operations and their potential cause of damage to underwater installations. The motion differential equations in the time domain was presented to predict the falling motion and some key parameters which have significant influence on the object motion were also carried out. Alessandro (2000) utilized a probabilistic methodology to estimate the pipeline impact and rupture frequencies related to dropped objects, thus may give useful information about the highest impact frequency location as well as the rupture frequency upstream and downstream of the valve. Yang et al. (2009) carried out experiments and numerical simulations, finding that the initial impact position influenced the impact results. Stefani et al. (2009) developed a new model to estimate the annual failure frequency

based on design and operating conditions and predict the level of risk to both human being and the environment. Stefani and Carr (2010) used Quantitative Risk Assessment (QRA) to predict the level of risk to see if there is a common trend regarding failure rates and failure-rate dependence on pipeline parameters. Xiang et al. (2016) considered a new three-dimensional (3D) theory which considers the effect of axial rotation on dropped cylindrical objects. Based on this 3D theory, a numerical tool called Dropped Objects Simulator (DROBS) had been developed to determine the risk-free zones for offshore lifting operations. Bin et al. (2016) used finite element analysis to analyze the impact damage of deck construction, equipment and subsea pipelines, obtain empirical formula through these data and finally construct failure function in Monte Carlo calculation to simplify the collision calculation. At the same time, in models involving many input variables, sensitivity analysis is an essential ingredient of model building and quality assurance. National and international agencies involved in impact assessment studies have included sections devoted to sensitivity analysis in their guidelines. Examples are the European Commission (see e.g. the guidelines for impact assessment) the White House Office of Management and Budget, the Intergovernmental Panel on Climate Change and US Environmental Protection Agency's modelling guidelines.

The proposed methodology of submarine pipeline failure probability assessment is shown in the flowchart below.

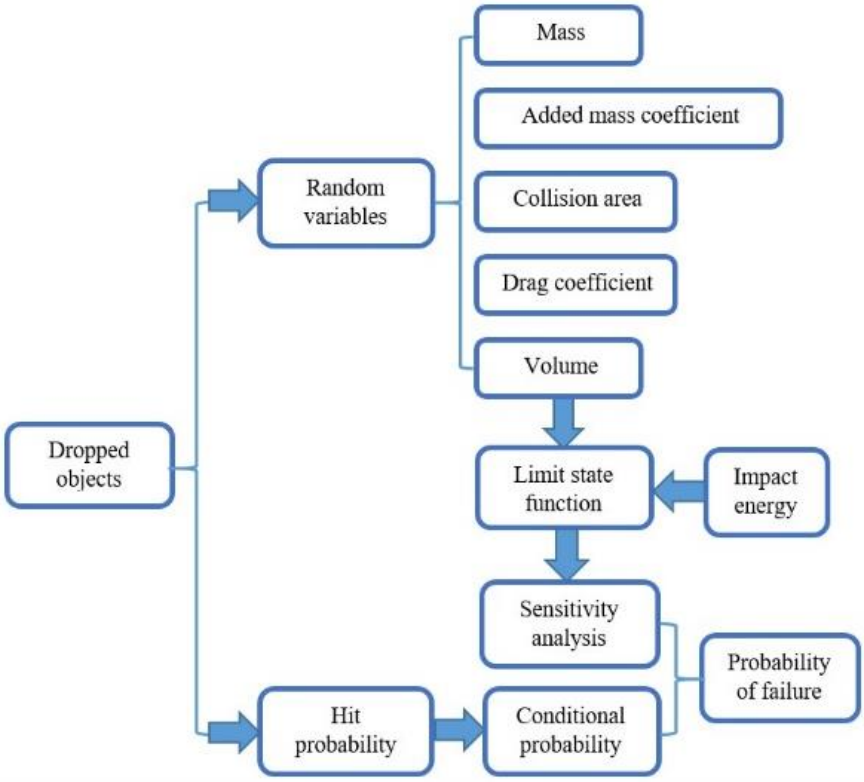

Figure 2 Proposed methodology of submarine pipeline failure probability assessment

In this paper, an example of a “detailed risk assessment of dropped objects on a 20-inch pipeline at seabed”, as described in DNV recommended practice rule is selected as the study case. Three different groups of flat/long shaped dropped objects (Case 1 ~ 3) and three different groups of box/round shaped dropped objects (Case 4 ~ 6) are used in the model with weights less than 2 tones (Case 1, Case 4), between 2 tones and 8 tones (Case 2, Case 5) and greater than 8 tones (Case 3, Case 6). The DNV simplified method is used to calculate the hit probability as well as the probability of failure in relation to impact frequency. The conditional hit probability for long/flat shaped objects will also be calculated with the method of an in-house tool **Dr**opped **Ob**jects **S**imulator (DROBS). The difference between the results of DNV rules and DROBS are also compared to see the pattern. Meanwhile, the sensitivity analysis convergent by Monte Carlo Simulation is also applied through MATLAB.

II. Theories

2.1 Risk Assessment Procedures in DNV's Recommended Practice

Since the excursion of different objects is a stochastic event, DNV's simplified method assumes the landing point on the horizontal position of seabed to be normally distributed:

$$p(x) = \frac{1}{\sqrt{2\pi}\delta} e^{-\frac{1}{2}\left(\frac{X}{\delta}\right)^2} \quad (1)$$

where, X is the horizontal position at the seabed (in 'meter'); δ is the lateral deviation (in 'meter') and $p(X)$ is the probability of a dropped object landing at position X.

The lateral deviation δ can be calculated based on the following formula:

$$\delta = d \cdot \tan\alpha \quad (2)$$

where, d is water depth.

The probability that a dropped object will land at the seabed within a certain distance R from the vertical line through the drop point is then expressed by the cumulative distribution function:

$$P(r \leq R) = \int_0^R p(r)dr \quad (3)$$

where, r is the absolute excursion on the seabed (in 'meter') and defined as $\sqrt{X^2 + Y^2}$; Y is the horizontal position along Y direction (in 'meter'); $p(r)$ is the probability of a dropped object landing at excursion r.

In DNV's guided practice, dropped objects can be classified into six types, as shown in Table 1.

Table 1 Object classification from DNV's guided practice

Description	Weight (tons)	Typical objects	Angular deviation α (°)
Flat/long shaped	< 2	Drill collar/casing, scaffolding	15
	2 – 8	Drill collar/casing	9
	> 8	Drill riser, crane boom	5
Box/round shaped	< 2	Container (food, space parts), basket, crane block	10
	2 – 8	Container (space parts), basket, crane test block	5
	> 8	Container (equipment), basket	3

The actual extent of the vulnerable items on the seabed within each ring can easily be incorporated by dividing the probability into several rings, as indicated in Fig. 3.

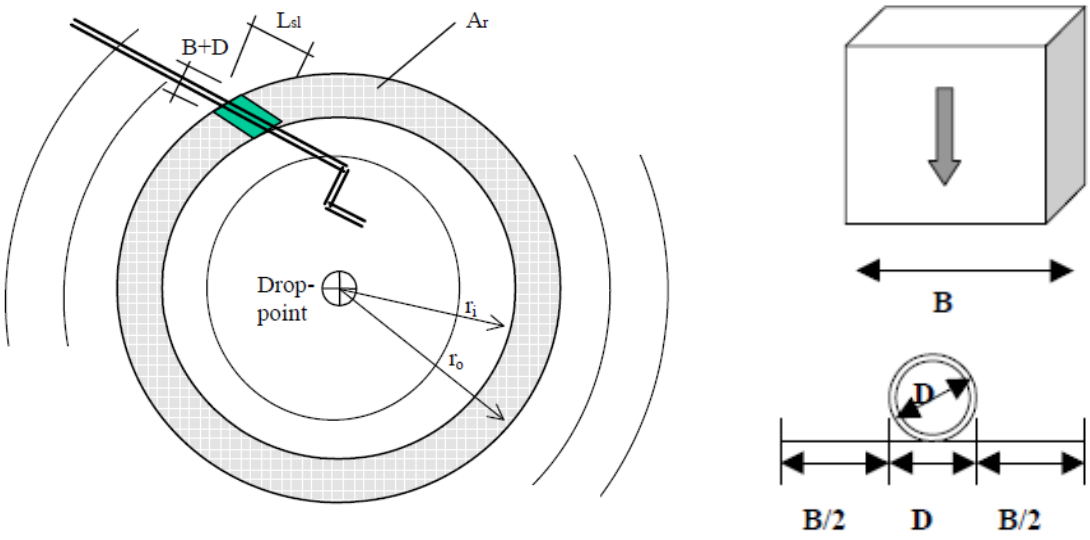

Figure 3 Probability of hit within a ring with inner radius r_i and outer radius r_o (DNV, 2010)

The probability of hit $P_{hit,r}$ within a ring area A_r with an inner radius r_i and an outer radius r_o can be found by:

$$P_{hit,r} = P(r_i < r \leq r_o) = P(r \leq r_o) - P(r \leq r_i) \tag{4}$$

The ring area A_r can be easily calculated by

$$A_r = \pi\left(r_o^2 - r_i^2\right) \tag{5}$$

The conditional probability of hit per seabed area, P_{hit,A_r}, is defined by dividing the hit probability $P_{hit,r}$ by the area of circle with radius r:

$$P_{hit,\ A_r,r} = \frac{P_{hit,r}}{A_r} \tag{6}$$

Within a certain ring, the probability of hit to a pipeline or umbilical with an object, $P_{hit,\mathrm{sl,r}}$, can be described as the exposed area which gives a hit within a ring divided on the total area of the ring, multiplied with the probability of hit within the ring, see Equation (7):

$$P_{hit,\mathrm{sl,r}} = P_{hit,r} \cdot \frac{L_{sl} \cdot (D+B)}{A_r} \tag{7}$$

where, $P_{hit,\mathrm{sl,r}}$ = Probability of hit on subsea line (sl) within a certain ring, r

$P_{hit,r}$ = Probability of hit within the ring, see Equation (4)

L_{sl} = length of subsea line within the ring (m)

D = Diameter of subsea line (m), see Fig. 3

B = Breadth of falling object (m), see Fig. 3

A_r= Area within the ring (m^2), see Fig. 3

The frequency of hit can be estimated based on the number of lifts, the drop frequency per lift and the probability of hit to the exposed sections of the subsea lines. For a certain ring around the drop point, the hit frequency is estimated by the following:

$$F_{hit,\mathrm{sl,r}} = N_{lift} \cdot f_{lift} \cdot P_{hit,\mathrm{sl,r}} \tag{8}$$

where, $F_{hit,\mathrm{sl,r}}$ = frequency of hit to the subsea line within a certain ring (per year)

N_{lift} = number of lifts (per year), see table 3

f_{lift} = frequency of drop per lift (per year), see table 2, and we use 1.2e-5 here

$P_{hit,\mathrm{sl,r}}$ = probability of hit to a subsea line within a certain ring, see Equation (7)

Table 2 Frequencies for dropped objects into the sea

Type of lift	Frequency of dropped object into the sea (per lift)
Ordinary lift to/from supply vessel with platform crane < 20 tones	1.2×10^{-5}
Heavy lift to/from supply vessel with the platform crane > 20 tones	1.6×10^{-5}
Handling of load < 100 tones with the lifting system in the drilling derrick	2.2×10^{-5}
Handling of BOP/load > 100 tones with the lifting system in the drilling derrick	1.5×10^{-3}

Table 3 Object classification of annual crane load data lifted

No	Description	Weight [tones]	Number lifted per year, N_{lift}
1	Flat/long shaped	< 2	700
2		2 – 8	50
3		> 8	5
4	Box/round shaped	< 2	500
5		2 – 8	2500
6		> 8	250

DNV's recommended practice, DNV-RP-107, should be the only guideline addressing the method to estimate the object excursion and hit probability. It provides a simple and efficient way to assess the risk of dropped objects in various offshore operations.

2.2 Damage classification in DNV's Recommended Practice

Damage situation is classified into three levels: minor damage (D1), moderate damage (D2) and major damage (D3). In case of a damage leading to release (D3), the following classification of releases are used: no release (R0), small release (R1), major release (R2), as shown in Fig. 4.

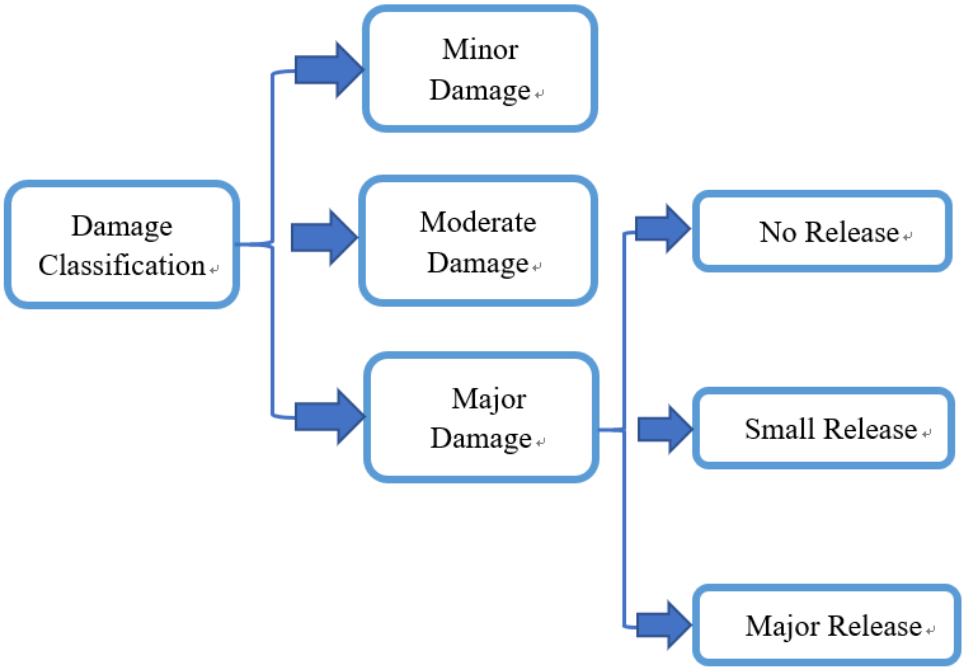

Figure 4 Damage classification to submarine pipelines

According to DNV guided rules, minor damage will not normally have any immediate influence of the operation of pipelines. Moderate damage usually need repair and major damage refers to the damage of pipeline ruptures. Since there is a rupture here, there will be some problems about contents release. Therefore, three release levels are offered from no release to major release. There is nothing special for no release level, which means that the hydrocarbon transported does not release from the pipeline. For small release, the pipeline may release small amount of contents from small to medium holes in the pipe wall (<80mm diameter). It will not stop until the hole is detected. Major release will lead to a total release of the content and will continue until the pipeline is isolated.

2.3 Energy analysis in DNV's Recommended Practice

For submarine pipelines, the energies they subject can be categorized into four genres, E_S – dent-absorbed energy for steel pipelines, E_E – the kinetic energy including terminal energy E_T and the energy of added hydrodynamic mass E_A, E_C – concrete coating energy, E_P – polymer coating energy.

While dropped objects finally hitting on the subsea pipelines, most impact are expected to result in a relatively "smooth" dent shape. The dent-absorbed energy relationship for steel pipelines are given as followed

$$\mathrm{E_s} = 16\left(\frac{2\pi}{9}\right)^{\frac{1}{2}} \cdot \mathrm{m_p} \cdot \left(\frac{\mathrm{D_0}}{\mathrm{t}}\right)^{\frac{1}{2}} \cdot \mathrm{D} \cdot \left(\frac{\delta}{\mathrm{D_0}}\right)^{\frac{3}{2}} \tag{9}$$

where, m_p = plastic moment capacity of the wall ($= \frac{1}{4}\sigma_y t^2$),

δ = pipe deformation (or dent depth),

t = wall thickness,

σ_y = yield stress,

$\mathrm{D_0}$ = steel outer diameter.

The plastic moment is defined as the moment at which the entire cross section has reached its yield stress. This is theoretically the maximum bending moment that the section can resist - when this point is reached a plastic hinge is formed and any load beyond this point will result in theoretically infinite plastic deformation.

The additional failure of punching through the wall, leading to leakage, can occur for higher velocity impacts or locally small and sharp impact geometry. The possibility of leakage and total rupture is included as a progressive conditional probability, where probability increases with increasing impact energy. The proposed damage classification used for bare steel pipes are shown in Table 4.

Table 4 Impact capacity and damage classification of steel pipelines and risers

Dent/ Diameter (%)	Damage description	Conditional Probability					
		D1	D2	D3	R0	R1	R2
<5	Minor damage	1	0	0	1	0	0
5-10	Major damage. Leakage anticipated.	0.1	0.8	0.1	0.9	0.1	0
10-15	Major damage. Leakage and rupture anticipated.	0	0.75	0.25	0.75	0.2	0.05
15-20	Major damage. Leakage and rupture anticipated.	0	0.25	0.75	0.25	0.5	0.25
>20	Rupture	0	0.1	0.9	0.1	0.2	0.7

For the kinetic energy E_E, we calculate the terminal velocity first with Equation (10) followed:

$$(\mathrm{m}-\mathrm{V}\rho)g=\frac{1}{2}\rho C_d A v_T^2 \tag{10}$$

Then, we could get the square of terminal velocity as:

$$v_T^2=\frac{2(m-V\rho)g}{\rho C_d A} \tag{11}$$

where, m = mass of dropped object,

V = volume of dropped object,

ρ = density of sea water,

A = collision area,

C_d = drag coefficient;

Since kinetic energy includes both terminal energy E_T and the energy of added hydrodynamic mass E_A, it can be written as:

$$E_E=E_T+E_A=\frac{1}{2}(m+m_a)v_T^2 \tag{12}$$

where, $m_a = \rho C_a V$,

C_a = added mass coefficient;

After substituting m_a and v_T^2 into Equation (12), we could easily obtain Equation (13) below:

$$E_E=\frac{g}{C_d A}\left(\frac{m^2}{\rho}-V.m+C_a V(m-V\rho)\right) \tag{13}$$

For concrete coating energy, different from DNV rules, E_C in this paper is chosen as the mean of the concrete coating energy for long/flat shaped objects E_{C1} and the concrete coating energy for box/round shaped objects E_{C2}.

$$E_{C1} = YB\frac{4}{3}\sqrt{Dx_0^3} \tag{14}$$

$$E_{C2} = YBhx_0 \tag{15}$$

$$E_c = \frac{E_{C1}+E_{C2}}{2} \tag{16}$$

where, Y = crushing strength,

B = width of the dropped object,

h = height of the dropped object;

x_0 = penetration depth, assume it is equal to wall thickness;

Fig. 5 gives a clearer view of the relationship between diameter and penetration depth.

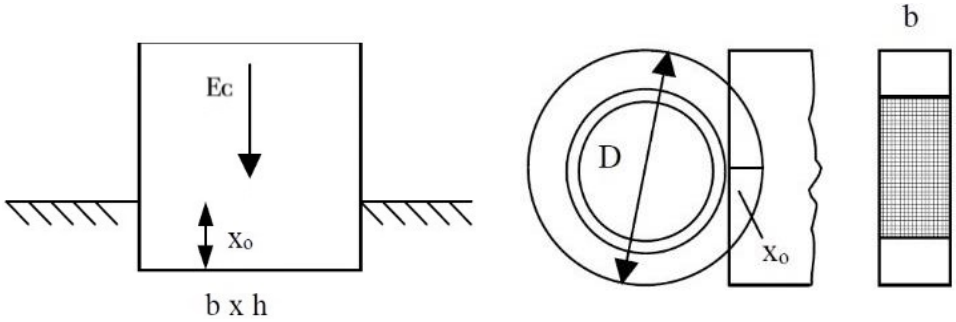

Figure 5 Impact in concrete coating (DNV, 2010)

According to DNV guide rule, the crushing strength should be 3 to 5 times of cube strength. As the cube strength varies typical from 35 to 45 MPa, here we use the middle point 40 MPa to calculate the energy. Similarly, the energy absorption in polymer coating is chosen as 15 kJ according to Table 5 since the concrete coating thickness of the dropped objects in this paper is 60mm.

Table 5 Energy absorption in polymer coating, E_P

Type of coating		Energy absorption
Corrosion coating with a thickness of maximum 3 – 6 mm.		~0 kJ
Thicker multi-layer coating (typical insulation coating with varying thickness)	6-15 mm	~5 kJ
	15-40 mm	~10 kJ
	>40 mm	~15 kJ
Mechanical protection systems (e.g. Uraduct)		5 kJ – 10 kJ

2.4 Basic theory for Dropped Objects Simulator (DROBS) in Two Dimensions (2D)

Dropped **Ob**jects **S**imulator – DROBS – is an in-house tool used to calculate the Equations of Motion (EOM) of cylindrical dropped objects. In his paper, it will be used to calculate the first three cases which will be mentioned later. For this in-house tool, two coordinate systems are used in the two-dimensional (2D) theory as shown in Fig. 6. OXZ is a global coordinate system in which the X-axis represents the stationary water surface and Z-axis points vertically above. The local coordinate system, which is denoted by oxz, is fixed on the cylinder with aligned x-axis. The origin of this local coordinate system is assumed to be located at the middle of dropped objects (Yu et al 2019).

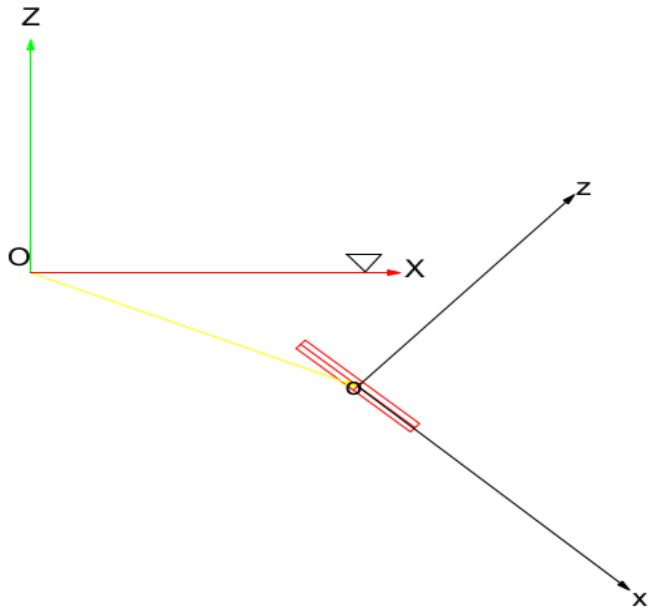

Figure 6 Coordinate systems for equations of motion in two dimensions (Yu et al 2019)

In this paper, the mass of dropped object is assumed to be uniformly distributed and the object itself is rigid and long/flat shaped in this method. Therefore, this kind of dropped objects will share the same mass center and geometric center.

According to Aanesland (1987), the falling process could be simplified into a two-dimensional problem considering only the motions in the x-z plane. The velocity components are U_1 (surge), U_3 (heave), and Ω_2 (pitch). The equations of motion are shown as followed:

$$(m-\rho\nabla)g\sin(\beta)+F_{dx}=m\dot{U}_1 \tag{17}$$

$$-(m-\rho\nabla)g\cos(\beta)+F_{dz}=\{U_1m_tU_3-U_1(x_tm_t)\Omega_2+m_{33}\dot{U}_3\}+m(\dot{U}_3-U_1\Omega_2) \tag{18}$$

$$M_{dy}+U_1(m_{33}+x_tm_t)U_3=U_1{x_t}^2m_t\Omega_2+m_{55}\dot{\Omega}_2+M_{55}\dot{\Omega}_2 \tag{19}$$

where, β = the instantaneous rotational angle between x-axis and X-axis,

m = mass of the cylinder,

M_{55} = moment of inertia in pitch direction,

m_{33} = added mass for heave motion from strip theory,

m_{55} = added mass for pitch motion from strip theory,

m_t = 2D added mass coefficient for heave direction at the trailing edge,

x_t = longitudinal position of effective trailing edge,

g = acceleration of gravity,

ρ = the density of sea water,

∇ = volume of the cylinder;

It should be noted that the motions in the above equations are stated in the body-fixed coordinate system oxz. Longitudinal position of effective trailing edge x_t is introduced because the ends of the cylinder are flat. Slender body theory assumes a smooth change in geometry, but the abrupt termination of the cylinder does not satisfy this condition. As shown in curly brackets on the right side of Equation (18) and (19), an additional force component is also included to account for trailing edge effect of the elongated elongate object (Newman, 1977). The other terms on the right side indicate inertial forces and moments.

In addition, viscous forces and moment, F_{dx}, F_{dz}, and M_{dy} are evaluated as followed:

$$F_{dx} = -0.664\pi D\sqrt{\nu\rho^2 L}U_1\sqrt{|U_1|} - \frac{1}{8}\rho\pi C_{dx}D^2U_1|U_1| \tag{20}$$

$$F_{dz} = 0.5\int_{-0.5L}^{0.5L}\rho C_{dz}DU_z(x)|U_z(x)|\,dx \tag{21}$$

$$M_{dy} = -0.5\int_{-0.5L}^{0.5L}\rho C_{dz}DxU_z(x)|U_z(x)|\,dx \tag{22}$$

The first term in Equation (20) represents the frictional drag which can be obtained from boundary layer theory for turbulent flow (Schlichting, 1979) and the second term represents a form drag component (Hoerner, 1958). Morison equation (Gudmestad et al, 1996) is used in Equation (21) and (22). The unknown parameter $U_z(x)$ is the local relative velocity in z-axis direction between cylinder and water. It could be represented as:

$$U_z(x) = -(U_3 - \Omega_2 x), \qquad -0.5L < x < 0.5L. \tag{23}$$

After submitting Equation (23) into Equation (21) and (22), we can obtain:

$$\begin{aligned} F_{dz} &= 0.5\int_{-0.5L}^{0.5L}\rho C_{dz}DU_z(x)|U_z(x)|\,dx \\ &= 0.5\rho C_{dz}D\int_{-0.5L}^{0.5L} -(U_3 - \Omega_2 x)|U_3 - \Omega_2 x|\,dx \end{aligned} \tag{24}$$

$$M_{dy} = -0.5 \int_{-0.5L}^{0.5L} \rho C_{dz} D x U_z(x) |U_z(x)| \, dx$$
$$= 0.5 \rho C_{dz} D \int_{-0.5L}^{0.5L} x(U_3 - \Omega_2 x) |U_3 - \Omega_2 x| \, dx \quad (25)$$

where, D = diameter of the cylinder,

ν = kinematic viscosity of water,

L = length of the cylinder,

C_{dx} = drag coefficient in x-direction,

C_{dz} = drag coefficient in z-direction;

In the numerical simulation, after solving U_1, U_3 and Ω_2 at each time step, the motions in the local coordinate system can be transformed into the motions in the global system by using this relationship below:

$$\begin{bmatrix} \dot{X} \\ \dot{Y} \end{bmatrix} = \begin{bmatrix} \cos(\beta) & -\sin(\beta) \\ \sin(\beta) & \cos(\beta) \end{bmatrix} \begin{bmatrix} U_1 \\ U_3 \end{bmatrix} \quad (26)$$

As axis Y and axis y are parallel, the inertial value$[X_0, Y_0] = [0,0]$, and $\dot{\beta} = \Omega_2$. Therefore, the rotation speed of the dropped cylinder around the axis Y and the axis y coincide (Yu et al 2019).

2.5 Failure probability analysis

In order to apply the sensitivity analysis, we use limit state function here. This is a concept related to a specified requirement is defined as a state of the structure including its loads at which the structure is just on the point of not satisfying the requirement (Ditlevsen. et al. 2005). The condition may refer to a degree of loading or other actions on the structure, while the criteria refer to structural integrity, fitness for use, durability or other design requirements. Therefore, the limit state function G is introduced into this paper defined as

$$G = L - S \tag{27}$$

where, L is the load that can be withstood by the property of the pipeline itself, S is the strength that comes from the dropped object. Fig. 7 illustrates the relationship between S and L as followed:

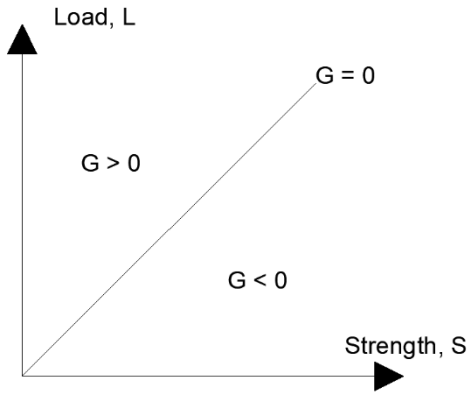

Figure 7 Failure space according to Equation (27)

The critical line for limit state is described by G = 0. When the strength is larger than pipeline load, failure takes place with G<0, similarly, the survival region is G>0. As a result, the probability of failure can be defined as Equation (28):

$$P_f = Pr(G \leq 0) = Pr(L \leq S) \tag{28}$$

According to Yong et al. (2014), the definition of probability of failure can be both qualitatively and quantitatively estimated as failure frequencies of different types of degradation mechanisms operating in the pipeline system. As a result, we define the probability of failure as followed:

$$POF = F_{hit,sl,r} \cdot P_{f,damage} \tag{29}$$

where, $F_{hit,sl,r}$ is frequency of hit to the subsea line within a certain ring (per year), see Equation (8). $P_{f,damage}$ is the probability of damage.

2.6 Sensitivity analysis adopted in Monte Carlo Simulation

According to limit state function in Equation (27), assume that both L and S follow Normal distribution, we could get:

$$L \sim N(\mu_L, \sigma_L^2)$$

$$S \sim N(\mu_S, \sigma_S^2)$$

Because of the nature of the normal distribution, we could easily obtain:

$$G \sim N(\mu_L - \mu_S, \sigma_L^2 + \sigma_S^2) \tag{30}$$

Let $\mu_G = \mu_L - \mu_S$, $\sigma_G = \sqrt{\sigma_L^2 + \sigma_S^2}$, we could normalize the function as followed:

$$\int_{-\infty}^{0} \mathrm{N}(\mathrm{G};\ \mu_G, {\sigma_G}^2)\,\mathrm{dG} = 1 \tag{31}$$

after which, we could get:

$$\frac{G-\mu_G}{\sigma_G} \sim N(0,1), G \leq 0 \tag{32}$$

As mentioned in section 2.3, E_E, E_S, E_C and E_P are four energies used to present the mean of the reliability, respectively. Let σ_{EE}, σ_{ES}, σ_{EC} and σ_{EP} to be the standard deviation of E_E, E_S, E_C and E_P, respectively. Since E_S, E_C and E_P are assumed to follow the normal distribution and each of the random variables corresponds to a certain value of E_E, a concept is recommended here as coefficient of variance (CV) to calculate σ_{EE}, σ_{ES}, σ_{EC} and σ_{EP} with equation followed:

$$\mathrm{CV} = \frac{\sigma}{\mu} \tag{33}$$

In probability theory and statistics, the coefficient of variation (CV) is a standardized measure of dispersion of a probability distribution or frequency distribution, which is often expressed as a percentage. The values of CV related to each energy is shown in Table 6.

Table 6 Values of coefficient of variance related to relevant energy

	E_S	E_C	E_P	E_E
coefficient of variance	5%	20%	20%	10%

Then σ_L^2 is calculated as:

$$\sigma_L^2 = {\sigma_{ES}}^2 + {\sigma_{EC}}^2 + {\sigma_{EG}}^2 \tag{34}$$

σ_S^2 is calculated as:

$$\sigma_S^2 = {\sigma_{EE}}^2 \tag{35}$$

The main impact from dropped object comes from kinetic energy. As most limit state situations are implicit, we use the thought of response surface method to transform the implicit function to explicit one, as mentioned by M. Jorge. Thus, neglecting the deformation of dropped objects, meanwhile, considering the impact energies absorbed completely by submarine pipelines, the limit state function can be rewritten as:

$$\begin{aligned} G &= (E_C + E_P + E_s) - E_E \\ &= (E_C + E_P + E_s) - \frac{g}{C_d A}\left(\frac{m^2}{\rho} - V.m + C_a V(m - V\rho)\right) \end{aligned} \tag{36}$$

As can be seen from the Equation (36), there are totally five random parameters, which is mass, volume, added mass coefficient, drag coefficient and collision area. In this paper, we will discuss the reliability sensitivity for all these five random variables. To fit the probability analysis, the following assumptions are used:

1. Mass follows uniform distribution between 1 to 10 tones as cranes have a limited capacity.
2. Volume follows normal distribution with mean $0.081m^3$ and standard deviation at $0.023m^3$.
3. The collision area between pipelines and dropped objects are determined by several reasons, which means the exact value of that cannot be predicted. Meanwhile, Yu et al. (2016) have proposed mass related upper and lower bounds for the minimum impact area (from 0.5 to 3), therefore truncated normal distribution is used to modeling collision area as a random variable.
4. Similarly, added mass coefficient and drag coefficient also follow truncated normal distribution, as according to DNV guide, C_a and C_d value between 0.1 to 1.5 and 0.7 to 1.5, respectively.

Table 7 shows the summary of the distribution types of random variables.

Table 7 Distribution types of random variables

Parameter	Distribution Type
Mass (m)	Uniform
Volume (V)	Normal
Collision Area (A)	Truncated Normal
Drag coefficient (C_d)	Truncated Normal
Add mass coefficient (C_a)	Truncated Normal

According to Papaioannou et al. (2010), for sensitivity analysis, we denote $\tilde{P}_f(\theta; \sigma)$ as an approximation of the probability of damage, expressed as Equation (37).

$$\tilde{P}_f(\theta, \sigma_G) = \int_{D(\boldsymbol{x})} \phi\left(-\frac{G(\boldsymbol{x};\theta)}{\sigma_G}\right) f_{\boldsymbol{X}}(\boldsymbol{x}) dx \tag{37}$$

where, X = an n-dimensional vector of random variables described by the joint PDF $f_X(x)$,

$f_X(x)$ = joint probability density function of random variables,

$D(x)$ = R^n, the set of all n-tuples of real numbers,

ϕ = standard normal cumulative distribution function,

θ = the parameter to which sensitivity analysis is performed,

G = limit state function;

The reason for integration on normal cumulative distribution is that this is a distribution based on the mean value. Taking the derivative of Equation (37) with respect to θ, and according to Leibniz integral rule we could rewritten Equation (37) as:

$$\frac{\partial \tilde{P}_f(\theta;\sigma_G)}{\partial \theta} = -\int_{D(\boldsymbol{x})} \frac{1}{\sigma_G} \varphi\left(\frac{G(\boldsymbol{x};\theta)}{\sigma_G}\right) \frac{\partial G(\boldsymbol{x};\theta)}{\partial \theta} f_{\boldsymbol{X}}(\boldsymbol{x}) dx \tag{38}$$

It should be noticed that since standard normal distribution is symmetric at the origin, the negative sign in ϕ function could be removed for symmetry of ϕ.

Finally, we use Monte Carlo samples $\{\boldsymbol{x_k}, k = 1, \dots\dots, n_s\}$ to simplify and estimate the domain integral in Equation (38), we can get:

$$\frac{\partial \tilde{P}_f(\theta;\sigma_G)}{\partial \theta} \approx \frac{1}{n_s} \sum_{k=1}^{n_s} \left[-\frac{1}{\sigma_G} \varphi\left(\frac{G(\boldsymbol{x_k};\theta)}{\sigma_G}\right) \frac{\partial G(\boldsymbol{x_k};\theta)}{\partial \theta}\right] \tag{39}$$

III. Case Study

3.1 Property of dropped objects and subsea pipelines

In this paper, the "detailed risk assessment of dropped objects on a 20-inch pipeline at seabed", as described in DNV recommended practice rule, is selected as the study case. Three different groups of flat/long shaped dropped objects (Case 1 ~ 3) and three different groups of box/round shaped dropped objects (Case 4 ~ 6) are used in the model with weights less than 2 tones (Case 1, Case 4), between 2 tones and 8 tones (Case 2, Case 5) and greater than 8 tones (Case 3, Case 6). The basic properties of the dropped objects and subsea pipelines are shown in the Table 8 and Table 9, respectively.

Table 8 Properties of dropped objects

Properties	Unit	
Length for long shape object (l)	m	12
Length for box shape object (l)	m	5
Height for impacting object (h)	m	0.3
Breadth for impacting object (b)	m	0.03
Gravity acceleration (g)	m/s^2	9.81

Table 9 Properties of subsea pipelines

Properties	Unit	
Pipeline diameter (D)	m	0.63
Wall thickness (t)	m	0.018
Concrete thickness (c)	m	0.06
Yield stress (s)	N/m^2	4.5e06

In addition, the frequency of dropped load into the sea is chosen as 1.2×10^{-5} per lift.

3.2 Field layout

The field layout is shown in Fig. 8. It can be seen that there are some areas of the subsea pipes shielded by the platform legs and bracing, within the range from 0m to 60m. That's why the pipeline length considered in the calculation of probability $P_{hit,\ A_r}$ should be zero in Table 10. Here, we just discuss the subsea layout from 0m to 100m, with water depth at 100m.

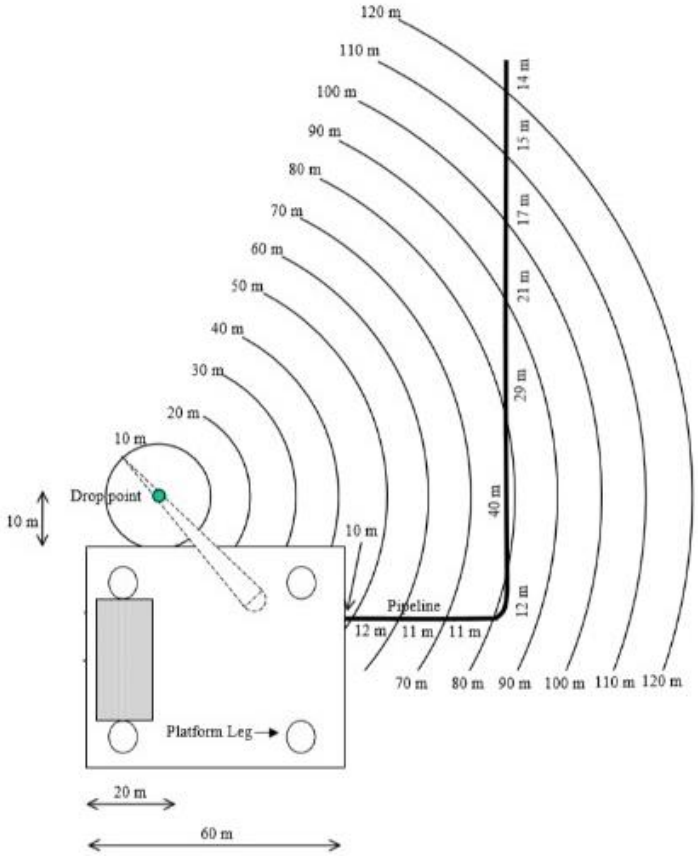

Figure 8 Field layout with 10-meter interval rings (DNV, 2010)

Table 10 Length of pipeline within each of 10-meter interval rings on the seabed

	Pipeline length within each ring									
	0m – 10m	10m – 20m	20m – 30m	30m – 40m	40m – 50m	50m – 60m	60m – 70m	70m – 80m	80m – 90m	90m – 100m
Length (m)	0	0	0	0	0*	0*	11	51	41	21

* Assumed shielded by the platform legs and bracing

IV. Results and Discussions

4.1 Hit Probability based on DNV rules

The pipeline diameter is 0.63m including coating and the object size is assumed to be 12-meter long for long/flat shaped objects and 5-meter long for box/round shaped objects. DNV rules had been used to calculate the hit probability within each ring. The results are shown in Table 11 as followed.

Table 11 Hit probability within each ring

Object			Hit probability within each ring [m^{-2}]				
no	Des.	Breadth (m)	0m – 10m	10m –20m	20m – 30m	30m – 40m	40m –50m
1	Flat/long shaped	12	9.26E-04	2.69E-04	1.23E-04	5.79E-05	2.60E-05
2		12	1.50E-03	3.41E-04	9.45E-05	2.12E-05	3.52E-06
3		12	2.38E-03	2.45E-04	1.38E-05	2.73E-07	1.70E-09
4	Box/round shaped	5	1.37E-03	3.33E-04	1.07E-04	2.98E-05	6.62E-06
5		5	2.38E-03	2.45E-04	1.38E-05	2.73E-07	1.70E-09
6		5	3.00E-03	5.97E-05	8.63E-08	4.72E-12	8.13E-18
Object			Hit probability within each ring [m^{-2}]				
no	Des.	Breadth (m)	50m – 60m	60m –70m	70m – 80m	80m –90m	90m – 100m
1	Flat/long shaped	12	1.07E-05	3.95E-06	1.31E-06	3.83E-07	9.93E-08
2		12	4.18E-07	3.47E-08	2.00E-09	7.98E-11	2.18E-12
3		12	3.17E-12	1.71E-15	1.88E-19	0.00E+00	0.00E+00
4	Box/round shaped	5	1.13E-06	1.46E-07	1.40E-08	1.01E-09	5.33E-11
5		5	3.17E-12	1.71E-15	1.88E-19	0.00E+00	0.00E+00
6		5	0.00E+00	0.00E+00	0.00E+00	0.00E+00	0.00E+00

To intuitively display the differences between these data, Fig. 9 plots a 3-D histogram to show the results of hit probability of dropped object within each ring.

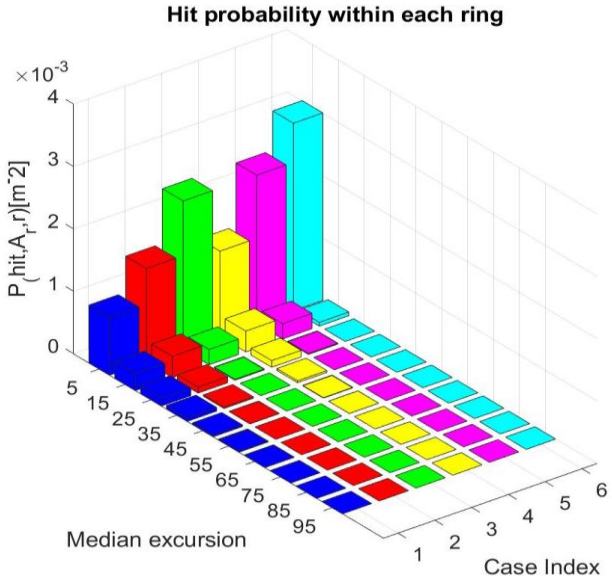

Figure 9 Hit probability with each ring

A similar trend could be seen from the Fig. 9 that, within the excursion around 0m to 30m, it is more likely for dropped objects to hit within each ring area. If we categorize these six cases into two groups – Case 1, 2, 3 and Case 4, 5, 6 – it will be apparent that hit probability increases as the mass of the dropped object increases. This is reasonable that generally, heavier objects are less affected by the outside environment than lighter ones in the same circumstance, since lighter objects are more likely to follow a "leaf" moment (Katteland et.al, 1995) when falling regardless of weights.

When water depth gets deeper, the probability gets smaller. This may be because that when the water is deep enough, the dropped object will obtain and maintain a terminal velocity before it hits within the ring area. This procedure will be more likely influenced by several outside environment conditions, like currents, waves etc.

Similarly, the conditional probability for dropped objects to hit the pipeline is calculated with same method. For each object to hit the pipeline within 10-meter intervals on the seabed, its conditional probability depends mainly on the results from the Table 10, the length of pipeline within each ring in Table 10, the pipeline diameter and object size in Table 8 as well as Table 9 and Equation (7). The results are shown in Table 12.

Table 12 Conditional probability for objects to hit the pipeline

Object			Conditional probability within each ring				
no	Des.	Breadth (m)	0m – 10m	10m –20m	20m – 30m	30m – 40m	40m –50m
1	Flat/long shaped	12	0.00E+00	0.00E+00	0.00E+00	0.00E+00	0.00E+00
2		12	0.00E+00	0.00E+00	0.00E+00	0.00E+00	0.00E+00
3		12	0.00E+00	0.00E+00	0.00E+00	0.00E+00	0.00E+00
4	Box/round shaped	5	0.00E+00	0.00E+00	0.00E+00	0.00E+00	0.00E+00
5		5	0.00E+00	0.00E+00	0.00E+00	0.00E+00	0.00E+00
6		5	0.00E+00	0.00E+00	0.00E+00	0.00E+00	0.00E+00
Object			Conditional probability within each ring				
no	Des.	Breadth (m)	50m – 60m	60m –70m	70m – 80m	80m –90m	90m – 100m
1	Flat/long shaped	12	0.00E+00	5.49E-04	8.42E-04	1.98E-04	2.63E-05
2		12	0.00E+00	4.82E-06	1.29E-06	4.13E-08	5.78E-10
3		12	0.00E+00	2.37E-13	1.21E-16	0.00E+00	0.00E+00
4	Box/round shaped	5	0.00E+00	9.02E-06	4.03E-06	2.32E-07	6.30E-09
5		5	0.00E+00	1.06E-13	5.41E-17	0.00E+00	0.00E+00
6		5	0.00E+00	0.00E+00	0.00E+00	0.00E+00	0.00E+00

As mentioned in Section 3.2, since areas from 0m to 60m of the subsea pipes are shielded by the platform legs and bracing, the conditional probability should be zero in those areas. A 3-D figure is also plotted to intuitive the data.

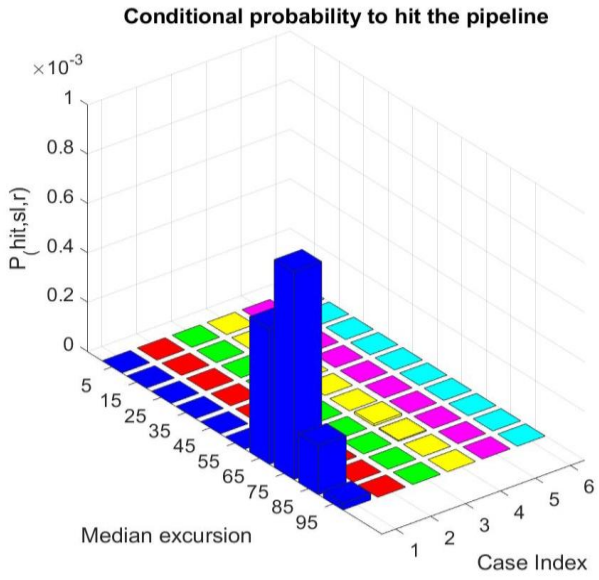

Figure 10 Conditional probability to hit the pipeline

Obviously, only Case 1 has the largest probability to hit on the subsea pipeline within excursion around 60m to 90m. Although box/round shaped objects have larger number lifted per year than long/flat shaped objects, the landing points for heavier objects are more likely to scatter close to the offshore platform. While for lighter objects, they will be affected by many other factors like currents etc. which will lead them to a further distance.

4.2 Hit probability based on DNV rules and DROBS

This in-house method can only be used to calculate the long/flat shaped dropped objects. As a result, we use properties of long/flat shaped objects from Case 1 to 3 as study cases. 1000 samples are used to calculate the hit probability and the conditional hit probability. We count the number of samples falling in certain ring area, and divided it by the total sample number to obtain the original hit probability. These results will be compared to those calculated by DNV rules method. The comparison of hit probability within each ring is shown in Table 13.

Table 13 Comparison of hit probability within each ring

Case Index	Method	Probability within each ring [m-2]				
		0m – 10m	10m –20m	20m – 30m	30m – 40m	40m –50m
Case 1	DNV	9.26E-04	2.69E-04	1.23E-04	5.79E-05	2.60E-05
	DROBS	2.48E-03	2.23E-04	7.64E-06	0.00E+00	0.00E+00
Case 2	DNV	1.50E-03	3.41E-04	9.45E-05	2.12E-05	3.52E-06
	DROBS	2.97E-03	7.11E-05	0.00E+00	0.00E+00	0.00E+00
Case 3	DNV	2.38E-03	2.45E-04	1.38E-05	2.73E-07	1.70E-09
	DROBS	3.18E-03	0.00E+00	0.00E+00	0.00E+00	0.00E+00
Case Index	Method	Probability within each ring [m-2] (Continued)				
		50m – 60m	60m –70m	70m – 80m	80m –90m	90m – 100m
Case 1	DNV	1.07E-05	3.95E-06	1.31E-06	3.83E-07	9.93E-08
	DROBS	0.00E+00	0.00E+00	0.00E+00	0.00E+00	0.00E+00
Case 2	DNV	4.18E-07	3.47E-08	2.00E-09	7.98E-11	2.18E-12
	DROBS	0.00E+00	0.00E+00	0.00E+00	0.00E+00	0.00E+00
Case 3	DNV	3.17E-12	1.71E-15	1.88E-19	0.00E+00	0.00E+00
	DROBS	0.00E+00	0.00E+00	0.00E+00	0.00E+00	0.00E+00

To intuitively display the differences between these data, Fig. 11 plots a 3-D histogram to show the difference between hit probabilities of dropped object within each ring.

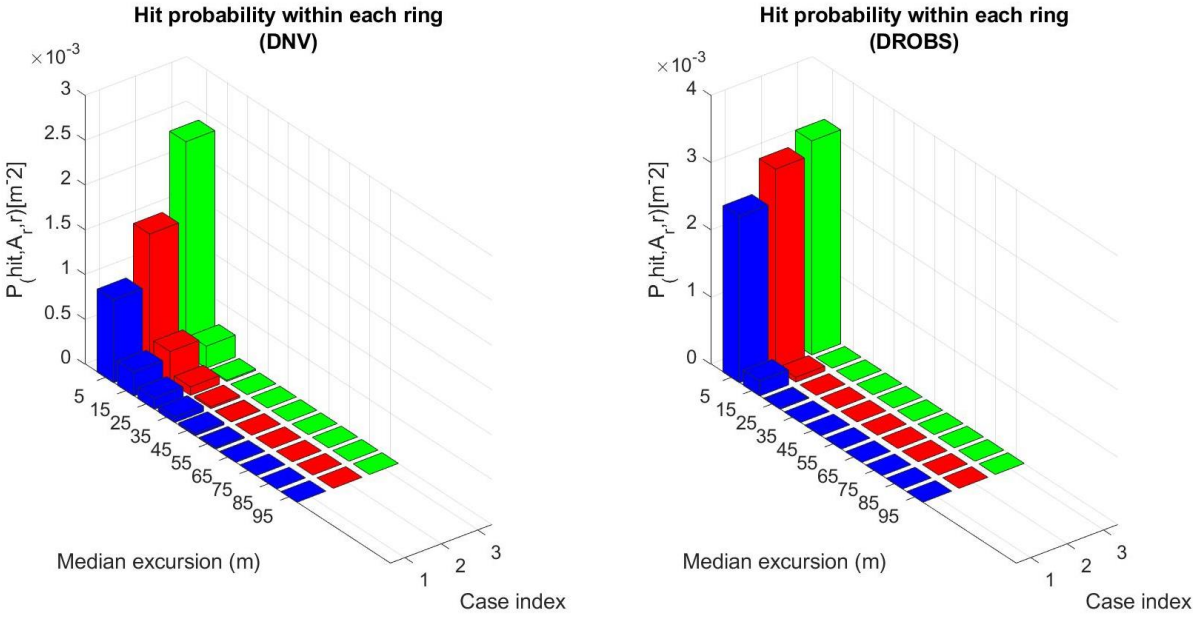

Figure 11 Results of hit probability within each ring from DNV (left) and DROBS (right)

Obvious difference could be seen from Fig. 11that Case 1 calculated by DROBS has a larger hit probability within each ring, approximately twice the result from DNV rules. The similarity is that, both of these two methods show the same number magnitude with a relatively dangerous excursion around 0m to 10 m, and the probability has same trend increasing with gradually increasing mass.

When it comes to conditional hit probability of dropped objects hitting on the subsea pipelines, the results are shown in Table 14 as followed:

Table 14 Conditional hit probability of dropped objects hitting on pipelines

Case Index	Method	Conditional probability of hitting the pipeline				
		0m – 10m	10m –20m	20m – 30m	30m – 40m	40m –50m
Case 1	DNV	0.00E+00	0.00E+00	0.00E+00	0.00E+00	0.00E+00
	DROBS	0.00E+00	0.00E+00	0.00E+00	0.00E+00	0.00E+00
Case 2	DNV	0.00E+00	0.00E+00	0.00E+00	0.00E+00	0.00E+00
	DROBS	0.00E+00	0.00E+00	0.00E+00	0.00E+00	0.00E+00
Case 3	DNV	0.00E+00	0.00E+00	0.00E+00	0.00E+00	0.00E+00
	DROBS	0.00E+00	0.00E+00	0.00E+00	0.00E+00	0.00E+00
Case Index	Method	Conditional probability of hitting the pipeline (Continued)				
		50m – 60m	60m –70m	70m – 80m	80m –90m	90m – 100m
Case 1	DNV	0.00E+00	5.49E-04	8.42E-04	1.98E-04	2.63E-05
	DROBS	0.00E+00	0.00E+00	0.00E+00	0.00E+00	0.00E+00
Case 2	DNV	0.00E+00	4.82E-06	1.29E-06	4.13E-08	5.78E-10
	DROBS	0.00E+00	0.00E+00	0.00E+00	0.00E+00	0.00E+00
Case 3	DNV	0.00E+00	2.37E-13	1.21E-16	0.00E+00	0.00E+00
	DROBS	0.00E+00	0.00E+00	0.00E+00	0.00E+00	0.00E+00

A 3-D plot is also plotted to intuitively distinguish the difference as shown in Fig. 12.

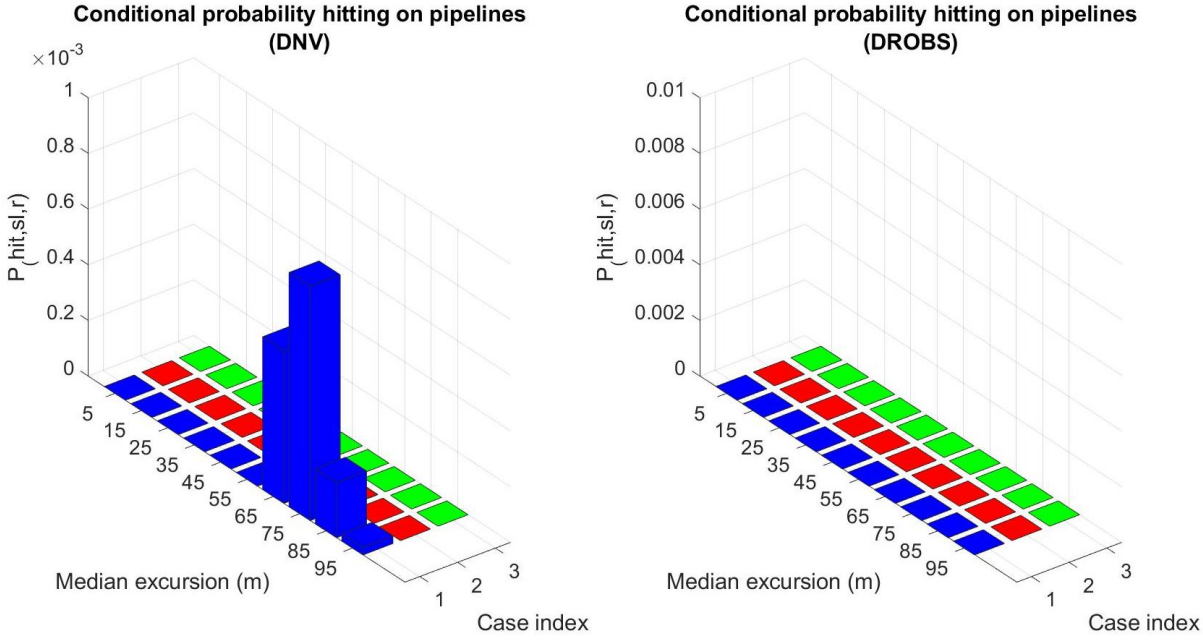

Figure 12 Results of conditional probability hitting on pipelines from DNV (left) and DROBS (right)

Since excursion from 0m to 60m is assumed to be shielded by offshore platform, the conditional probability of hitting on the subsea pipelines should be zero. However, based on DROBS' results of hit probability within each ring, excursion from 60m to 100m also shows no probability for all three cases.

4.3 Hit probability based on DNV rules and DROBS without platform shielded

We assume that the subsea pipelines are not shielded by the offshore platform to see the difference between the results from these two method. Then, the layout of pipelines will be changed into Table 15 as followed:

Table 15 Length of pipeline within each of 10-meter interval rings on the seabed without shielded

	Pipeline length within each ring without shielded									
	0m – 10m	10m – 20m	20m – 30m	30m – 40m	40m – 50m	50m – 60m	60m – 70m	70m – 80m	80m – 90m	90m – 100m
Length (m)	10	10	10	10	10	12	11	51	41	21

Therefore, we could get another group of conditional probability of hitting the pipeline shown in Table 16.

Table 16 Conditional probability of hitting the pipeline (without shielded)

Case Index	Method	Conditional probability of hitting the pipeline without shielded				
		0m – 10m	10m –20m	20m – 30m	30m – 40m	40m –50m
Case 1	DNV	1.17E-01	3.40E-02	1.55E-02	7.32E-03	3.28E-03
	DROBS	3.13E-01	2.81E-02	9.65E-04	0.00E+00	0.00E+00
Case 2	DNV	1.90E-01	4.30E-02	1.19E-02	2.68E-03	4.45E-04
	DROBS	3.75E-01	8.98E-03	0.00E+00	0.00E+00	0.00E+00
Case 3	DNV	3.00E-01	3.09E-02	1.74E-03	3.45E-05	2.15E-07
	DROBS	4.02E-01	0.00E+00	0.00E+00	0.00E+00	0.00E+00
Case Index	Method	Conditional probability of hitting the pipeline without shielded (Continued)				
		50m – 60m	60m –70m	70m – 80m	80m –90m	90m – 100m
Case 1	DNV	1.62E-03	5.49E-04	8.42E-04	1.98E-04	2.63E-05
	DROBS	0.00E+00	0.00E+00	0.00E+00	0.00E+00	0.00E+00
Case 2	DNV	6.33E-05	4.82E-06	1.29E-06	4.13E-08	5.78E-10
	DROBS	0.00E+00	0.00E+00	0.00E+00	0.00E+00	0.00E+00
Case 3	DNV	4.81E-10	2.37E-13	1.21E-16	0.00E+00	0.00E+00
	DROBS	0.00E+00	0.00E+00	0.00E+00	0.00E+00	0.00E+00

3-D figure is shown as followed:

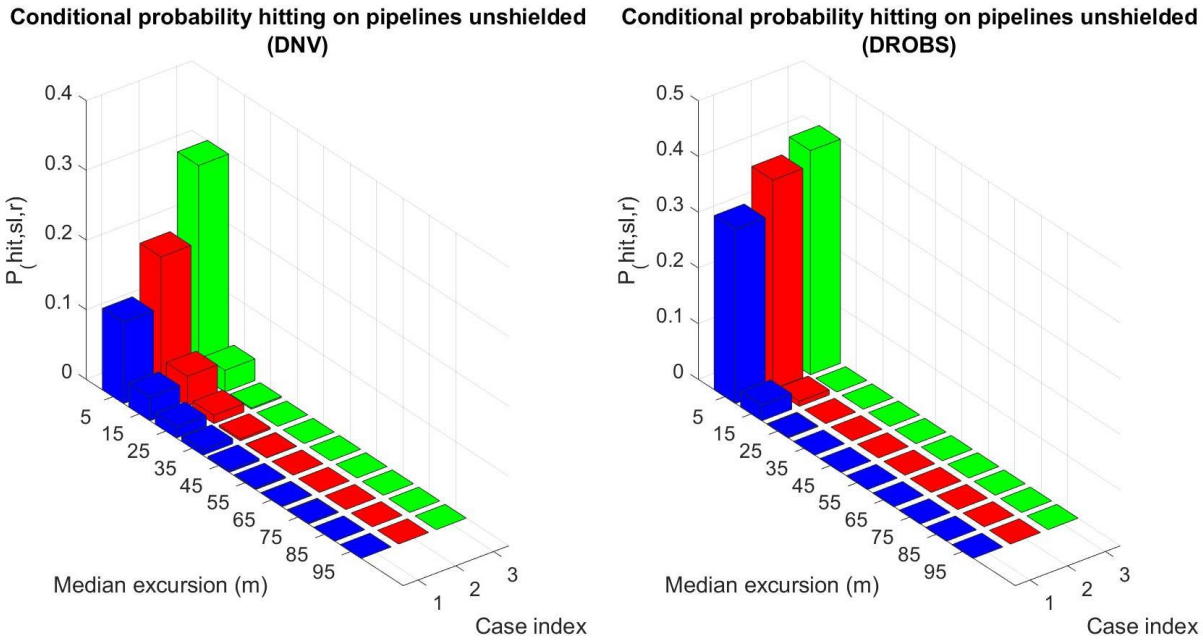

Figure 13 Conditional probability of hitting on subsea pipelines unshielded

It can be seen the shape of histogram are almost the same as that in Fig. 11. However, it should be noted that the magnitude of results are much larger. This is reasonable because if there is no shield over subsea pipeline from 0m to 60m, heavier dropped objects will have larger probability to cause damage.

There is still some difference between the results of two methods, especially for Case 1. The reason may be because that the estimation of lateral deviation δ based on Equation (2) is a purely empirical estimation, which completely neglects the effects of hydrodynamic coefficients (Awotahegn, 2015). Since DROBS takes the complex hydrodynamic coefficients into account, it may be more reliable especially on lighter objects.

4.4 Probability of damage

The probability of damage in Table 17 is calculated on the behalf of dropped objects with weight less than 10 tones.

Table 17 Probability of failure and damage

Different levels of damage	Impact energy		Damage probability	Conditional probability of failure, POF (normalized)		
	Steel pipe	Total		D1	D2	D3
Level 1	<15	<65	0.4661	6.37E-06	0	0
Level 2	15 - 40	65 - 90	0.0770	1.05E-07	8.41E-07	1.05E-07
Level 3	40 - 75	90 - 125	0.0825	0	8.46E-07	2.82E-07
Level 4	75 - 115	125 - 165	0.0439	0	1.50E-07	4.50E-07
Level 5	> 115	> 165	0.3304	0	4.51E-07	4.06E-06

Damage levels here are related with the ratio of dent over diameter of pipelines in Table 4, which can be reorganized into Table 18 as followed:

Table 18 Different damage level corresponding to different ratio

Different levels of damage	Dent /Diameter δ / D (%)
Level 1	< 5
Level 2	5 - 10
Level 3	10 - 15
Level 4	15 - 20
Level 5	> 20

D1, D2, D3 is damage classification mentioned in section 2.2 as minor damage, moderate damage and major damage. The figure of conditional probability of failure versus damage level is shown as followed:

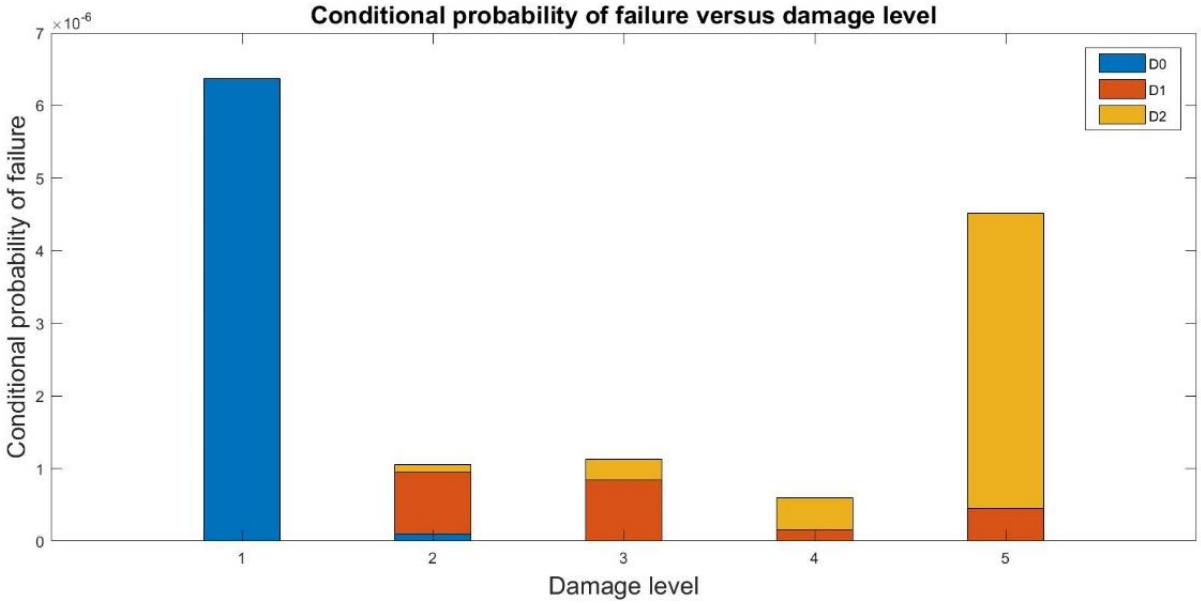

Figure 14 Conditional probability of failure versus damage level

It can be seen that minor damage almost occurs at damage Level 1 with little dent mark. Since major damage will cause large influence on subsea pipeline, it is reasonable for it to happen mostly on damage Level 5 with more than 20% dent eruption.

From the table we could see that damage Level 1 has the highest probability at 46.61% followed by Level 5 at 33.04%. This result makes sense that although about 38% third party damage occurs every year, those who cause large casualty and losses are not much. As a result, damage Level 1 - damage neither requiring repair, nor resulting in any release of hydrocarbons - occurs frequently.

4.5 Results for reliability sensitivity analysis

The results of reliability sensitivity analysis with Monte Carlo Simulation for the probability of failure related to four random variables are calculated in MATLAB. To preliminarily obtain the normalized results, we randomly select 10000 different data of mass, volume, collision area, added mass coefficient and drag coefficient, respectively. The trend of change in variables' sensitivity has been shown from Fig. 15 to Fig. 19. The horizontal axis shows the parameter to which sensitivity analysis is performed and the vertical axis shows the extent to which the relevant parameter affects the probability of failure, which is $\frac{\partial \tilde{P}_f(\theta;\sigma_G)}{\partial \theta}$ in Equation (39). In Fig. 15, it is written as $d\mathrm{P_f}/d\mathrm{m}$; in Fig. 16, the vertical axis represents $d\mathrm{P_f}/d\mathrm{C_a}$; in Fig. 17, the vertical axis represents $d\mathrm{P_f}/d\mathrm{A}$; in Fig. 18, the vertical axis represents $d\mathrm{P_f}/d\mathrm{C}_d$; in Fig. 19, the vertical axis represents $d\mathrm{P_f}/d\mathrm{V}$. Meanwhile, the relevant data results will be shown in Table 19 to Table 23.

After analyzing the figures obtained below, we can categorize these five random variables into two groups, one for mass and added mass coefficient, and the other for collision area, drag coefficient and volume. Some conclusions can be made that for variable mass, it perfectly follows normal distribution. This makes sense that light dropped objects are more likely to cause minor damage related to Level 1. When mass increases, Level 5 will be more sensitive than the other Levels, as heavier objects will cause larger damages. Added mass coefficient, on the other hand, may have little influence on the whole system, since the sensitivity of it shows a nearly flat line pattern. According to Equation (36), as drag coefficient and collision area are both on the denominator, they are considered to have similar trend pattern.

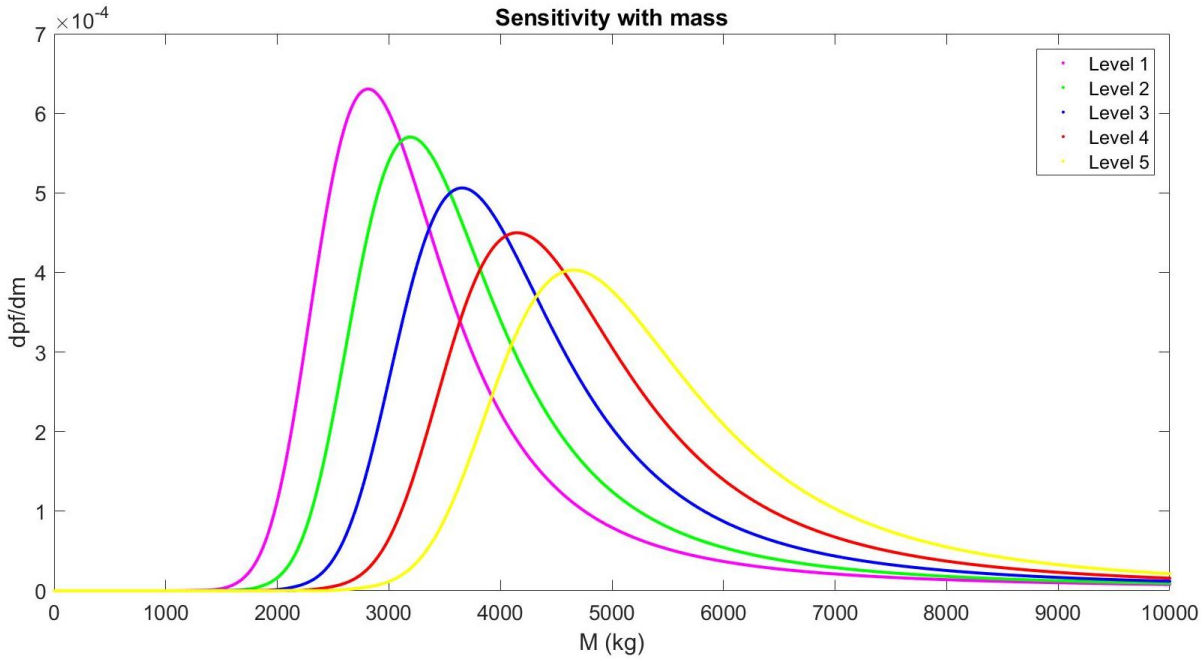

Figure 15 Sensitivity with mass

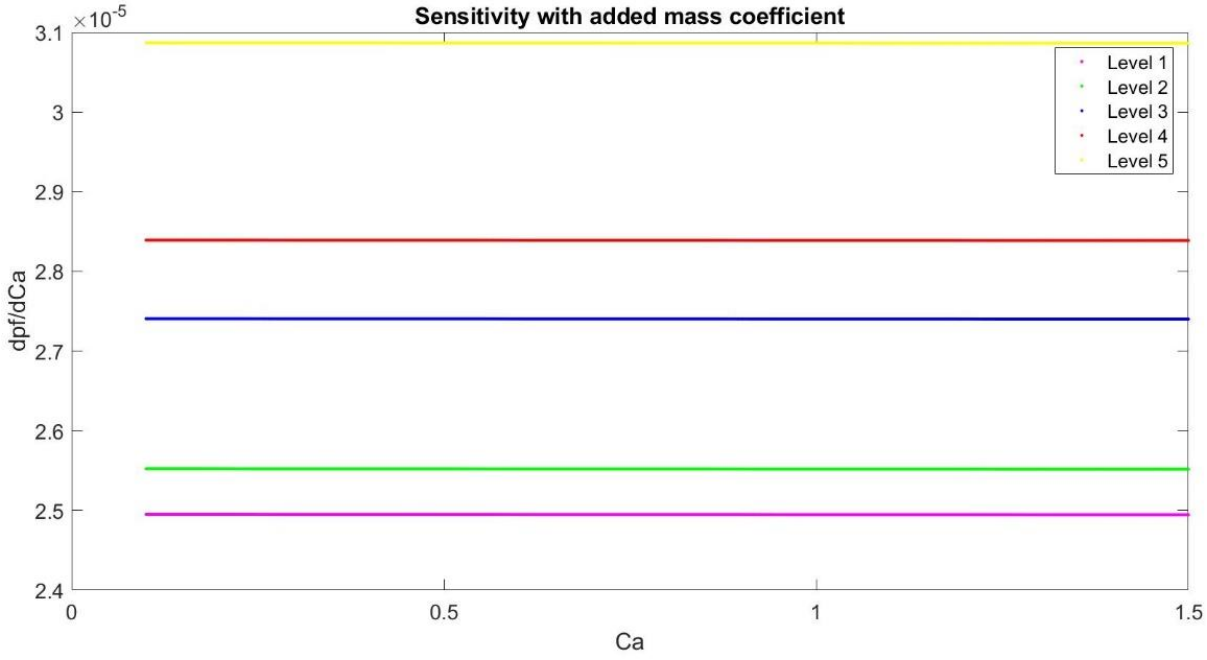

Figure 16 Sensitivity with added mass coefficient

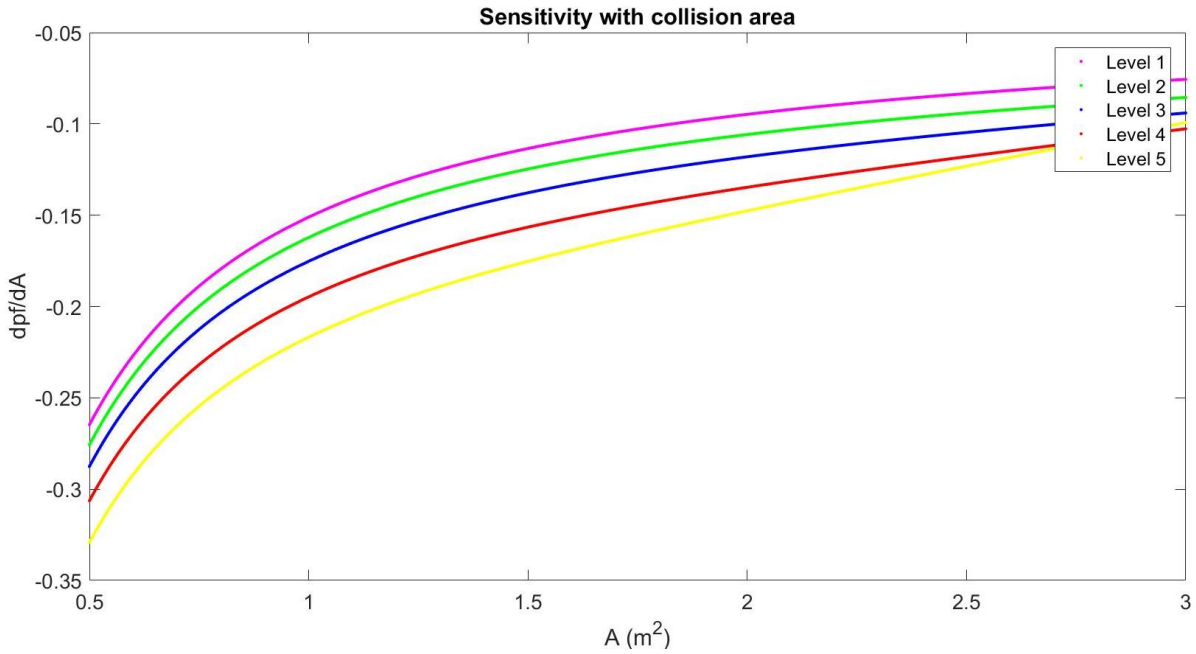

Figure 17 Sensitivity with collision area

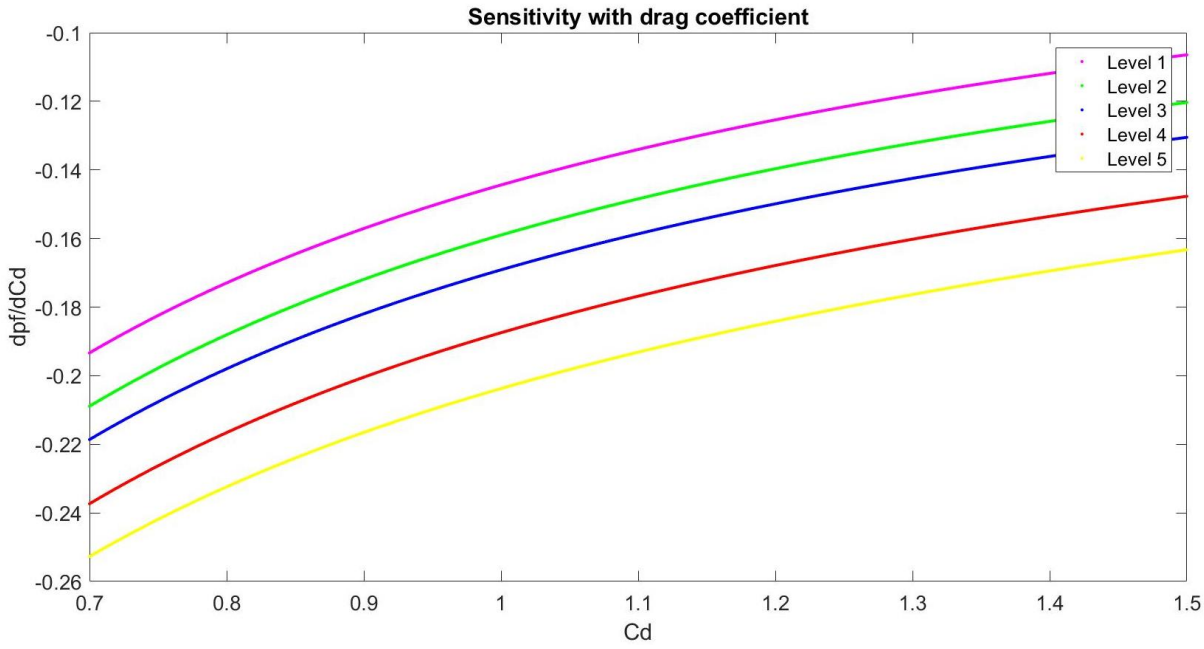

Figure 18 Sensitivity with drag coefficient

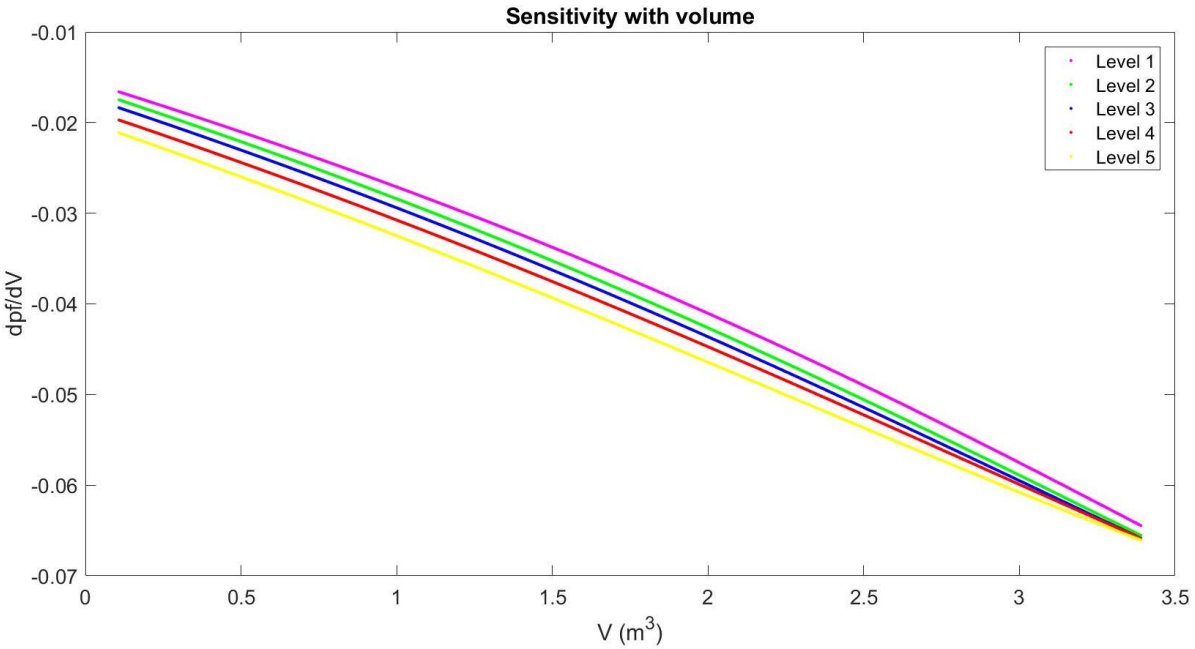

Figure 19 Sensitivity with volume

Detailed data for these figures are shown in tables followed:

Table 19 Data for sensitivity analysis on mass

M	1000	2000	4000	6000	8000	10000
Level 1	2.7454E-76	5.6940E-05	2.1838E-04	3.2455E-05	1.1812E-05	6.5221E-06
Level 2	5.9566E-160	8.1394E-06	3.4875E-04	4.9393E-05	1.5641E-05	7.9123E-06
Level 3	0.0000E+00	1.1101E-06	4.8410E-04	8.2254E-05	2.2561E-05	1.0248E-05
Level 4	0.0000E+00	7.6930E-11	4.6136E-04	1.3662E-04	3.3930E-05	1.3819E-05
Level 5	0.0000E+00	1.5896E-22	2.6757E-04	2.1132E-04	5.1602E-05	1.9085E-05

Table 20 Data for sensitivity analysis on added mass coefficient

Ca	0.1	0.28	0.46	0.64	0.82	1
Level 1	2.4597E-05	2.4597E-05	2.4596E-05	2.4596E-05	2.4595E-05	2.4595E-05
Level 2	2.5685E-05	2.5685E-05	2.5684E-05	2.5683E-05	2.5683E-05	2.5682E-05
Level 3	2.7359E-05	2.7359E-05	2.7358E-05	2.7358E-05	2.7357E-05	2.7356E-05
Level 4	2.8436E-05	2.8435E-05	2.8435E-05	2.8434E-05	2.8433E-05	2.8433E-05
Level 5	3.1576E-05	3.1575E-05	3.1575E-05	3.1574E-05	3.1573E-05	3.1572E-05

Table 21 Data for sensitivity analysis on collision area

A	0.5	1	1.5	2	2.5	3
Level 1	-0.2618	-0.1488	-0.1113	-0.0927	-0.0814	-0.0737
Level 2	-0.2718	-0.1598	-0.1228	-0.1042	-0.0926	-0.0842
Level 3	-0.2888	-0.1767	-0.1395	-0.1201	-0.1071	-0.0967
Level 4	-0.3055	-0.1930	-0.1544	-0.1324	-0.1157	-0.1007
Level 5	-0.3303	-0.2169	-0.1750	-0.1472	-0.1225	-0.0985

Table 22 Data for sensitivity analysis on drag coefficient

Cd	0.7	0.86	1.02	1.18	1.34	1.5
Level 1	-0.1936	-0.1640	-0.1430	-0.1277	-0.1161	-0.1070
Level 2	-0.2101	-0.1797	-0.1582	-0.1426	-0.1307	-0.1214
Level 3	-0.2186	-0.1890	-0.1680	-0.1528	-0.1412	-0.1320
Level 4	-0.2319	-0.2025	-0.1815	-0.1661	-0.1543	-0.1448
Level 5	-0.2531	-0.2236	-0.2024	-0.1867	-0.1743	-0.1640

Table 23 Data for sensitivity analysis on volume

V	0.11	0.76	1.42	2.07	2.73	3.39
Level 1	-0.0166	-0.0241	-0.0327	-0.0421	-0.0529	-0.0645
Level 2	-0.0175	-0.0253	-0.0341	-0.0437	-0.0544	-0.0655
Level 3	-0.0184	-0.0263	-0.0351	-0.0447	-0.0551	-0.0658
Level 4	-0.0197	-0.0277	-0.0364	-0.0458	-0.0558	-0.0658
Level 5	-0.0212	-0.0293	-0.0382	-0.0475	-0.0570	-0.0661

V. Conclusions

In this project, a sample field layout introduced in DNV recommended practice rule is selected as the study case. To better prevent the subsea systems from the damages caused by dropped objects, the conditional probability of failure and damage for dropped objects hitting on the pipelines is calculated. For the probabilities of long/flat shaped objects, both methods of DNV rules and DROBS are used. With Monte Carlo Simulation in MATLAB, the sensitivity analysis is used to study the influence of five random variables, which are mass, collision area, volume, added mass coefficient and drag coefficient.

For the case discussed in the Appendix of DNV (2010), the sum of the conditional probability of failure is 7.188e-06, which is within the acceptance criteria of 1E-05. This result indicates that for either long/flat shaped dropped objects or box/round shaped objects, the structures and coatings of the pipelines may absorb some energy to protect the system from damage.

For the probability of damage, Level 1 has the maximum likelihood to damage the submarine pipelines at 46.61%, followed by Level 5 of the probability of damage at 33.04%. It is reasonable that, in general, most of the things falling from cranes and offshore platforms weigh less than 2 tons, which explains the reason for the occurrence of probability of damage on Level 1. For damage Level 5, it can be explained that once large dropped objects (weight around 9 tones, for instance) hit on the pipeline, they will have larger chances to cause rupture.

For the reliability sensitivity analysis, Fig. 15 clearly shows that the lighter objects are more likely to cause minor damage, and the heavier objects may cause larger damages. This is why the curves for Level 1, Level 2, Level 3, Level 4 and Level 5 are sequentially arranged from left to right as the mass. Overall, the probability of damage is very sensitive to the mass. However, it may not be so sensitive to the change of the added mass coefficient C_a, because the sensitivity curves with C_a are almost nearly flat lines, as indicated in Fig. 16. Finally, considering that both the drag coefficient C_d and collision area A are given in the denominator in Equation (36), they both should have very similar pattern, as indicated by Figure 17 and Figure 18.

Reference

A. Mazzola (2000). A Probabilistic Methodology for the Assessment of Safety from Dropped Loads in Offshore Engineering. Risk Analysis, Vol. 20, No. 3.

B. Yu, L. Sun, S. Li, and X. Zhang (2016). The Improved Method of Risk Assessment for Falling Objects from the Crane of FPSO, OMAE2016, 54216, 1–8.

Det Norske Veritas (1988) “Design Guidance for Offshore Steel Structures Exposed to Accidental Loads”, DNV Report no. 88-3172.

Det Norske Veritas (DNV), 2010. DNV Recommended Practice: Risk assessment of pipeline protection, DNV-RP-F107.

D. Begg, D. Fox (1992). Dropped object risk assessment. Brighton and Portsmouth Polytechnic, U.K. Computer Modelling of Seas and Coastal Regions, Computational Mechanics Publications 1992, Page 507-522.

European Commission (2019). Impact Assessment Guidelines. January 15, SEC (2009) 92.

G. Xiang, L. Birk, X. Yu, H. Lub (2017). Numerical study on the trajectory of dropped cylindrical objects. Ocean Engineering 130(2017)1-9

H. Ghassemi, E. Yari (2011). The added mass Coefficient computation of sphere, ellipsoid and marine propellers using Boundary Element Method. POLISH MARITIME RESEARCH 1(68) 2011 Vol 18; pp. 17-26, 10.2478/v10012-011-0003-1.

H. Schlichting (1979). Boundary layer theory. McGraw-Hill Book Company, New York, USA.

I. Papaioannou, K. Breitung & D. Straub (2010). Reliability Sensitivity Analysis with Monte Carlo Methods. Engineering Risk Analysis Group Technische, Universit¨at M¨unchen, Munich, Germany

J. Yang, G. Lu, T. Yu, S. Reid (2009). Experimental study and numerical simulation of pipe-on-pipe impact. Int. J. Impact Eng., 36(10): 1259-1268.

J. Miranda. Structural reliability analysis with implicit limit state functions. Instituto Superior Tecnico, university of Lisbon, Portugal.

J. Newman (1977). Marine hydrodynamic. The MIT Press, Cambridge, Massachusetts, USA.

K. Breitung (1989). Asymptotic approximations for probability integrals. Probabilistic Engineering Mechanics, Vol. 4, No. 4, 1989 Computational Mechanics Publications.

L. Katteland, B. Hygarden (1995). Risk analysis of dropped objects for deep water development. OMAE 1995, 14th Intl Conf on Offshore Mechanics & Arctic Engng; 18-22 June 1995; Copenhagen, Denmark.

M. Awotahegn (2015). Experimental Investigation of Accidental Drops of Drill Pipes and Containers, Master's Thesis, University of Stavanger, Stavanger, Norway.

O. Ditlevsen, H. Madsen (2005). Structure reliability methods. Technical University of Denmark.

S. Edmollaii, P. Edalat, M. Dyanati (2019). Reliability Sensitivity Analysis of Dropped Object on Submarine Pipelines. Ocean Systems Engineering Volume 9, Number 2, 06-2019, pages 135-155.

S. Taghizadeh, P. Edalat (2017). Accidental Limit State of Submarine Pipeline: Trawl Gears Pull-Over Loads and Effect of Free Span. International Journal of Maritime Technology, IJMT Vol.8/ Summer 2017 (47-58).

S. Hoerner (1958). Fluid dynamics drag. Bricktown, NJ, USA.

V. Stefani, Z. Wattis, M. Acton (2009). A Model to Evaluate Pipeline Failure Frequencies based on Design and Operating Conditions. Global Congress on Process Safety. April 26-30, 2009, Tampa, FL, (USA). Proceedings, Page 210-229.

V. Stefani, P. Carr (2010). A model to estimate the failure rates of offshore pipelines. IPC2010-31230, Proceedings of IPC2010 8th International Pipeline Conference September 27-October 1, 2010, Calgary, Alberta, Canada.

V. Aanesland, A/S Marintek (1987). Numerical and experimental investigation of accidentally falling drilling pipes, 19th Annual OTC in Houston, Texas.

X. Yu, H. Meng, Y. Zhen, L. Li (2019). Trajectory prediction of cylinders freely dropped into water in two dimensions based on state space model. Ocean Engineering 187 (2019) 106154.

X. Yu, A. Steven, L. Li, Z. Xiong, H. Kang (2018). On the hit probability of freely falling cylindrical objects onto the pipeline at seabed. 11th International Conference on Marine Technology, MARTEC 2018.

Y. Luo, & J. Davis. (1992). Motion Simulation and Hazard Assessment Of Dropped Objects. London.

Y. Yang, F. Khan, P. Thodi, R. Abbassi (2016). Corrosion induced failure analysis of subsea pipelines. Reliability Engineering System Safety 159, DOI: 10.1016/j.ress.2016.11.014.

Y. Bai, Q. Bai (2014). Risk-based inspection. Subsea pipeline integrity and risk management.

VITA

The author was born in Shanghai, China. She obtained her bachelor's degree at the Department of Naval Architect and Marine Engineering, Shanghai Maritime University in June 2018. She was enrolled into UNO's NAME graduate program to pursue the master degree.